Analytica Chimica Acta
January 2022, Volume 1191, Pages 339212 (9p.)
https://doi.org/10.1016/j.aca.2021.339212
https://archimer.ifremer.fr/doc/00732/84409/

Prediction of fatty acids composition in the rainbow trout *Oncorhynchus mykiss* by using Raman micro-spectroscopy

Prado Enora [1], Eklouch-Molinier Christophe [2, *], Enez Florian [2], Causeur David [3], Blay Carole [4], Dupont-Nivet Mathilde [4], Labbe Pierre [5], Petit Vincent [6], Moreac Alain [7], Taupier Grégory [1], Haffray Pierrick [3], Bugeon Jérôme [8], Corraze Geneviève [9], Nazabal Virginie [1, *]

[1] CNRS, ISCR – UMR 6226, ScanMAT – UMS 2001, Univ Rennes, 35000, RENNES, France
[2] SYSAAF, Station LPGP-INRA, 35042, Rennes, France
[3] IRMAR UMR CNRS 6625, Agrocampus Ouest, Rennes Cedex, France
[4] Université Paris-Saclay, INRAE, AgroParisTech, GABI, Jouy-en-Josas, France
[5] INRAE, UE 0937, PEIMA, 29450, Sizun, France
[6] Les Sources de L'Avance, 40410, Pissos, France
[7] IPR – UMR 6251, Univ Rennes, 35000, RENNES, France
[8] INRAE, UR1037, LPGP, 35000, Rennes, France
[9] INRAE, Univ Pau & Pays Adour, E2S UPPA, UMR1419 NuMéA, 64310, Saint Pée, France

* Corresponding authors :
Christophe Eklouch-Molinier, email address : christophe.eklouh-molinier@inrae.fr ;
Virginie Nazabal, email address : virginie.nazabal@univ-rennes1.fr

Abstract :

The importance of poly-unsaturated fatty acids (PUFAs) in food is crucial for the animal and human development and health. As a complementary strategy to nutrition approaches, genetic selection has been suggested to improve fatty acids (FAs) composition in farmed fish. Gas chromatography (GC) is used as a reference method for the quantification of FAs; nevertheless, the high cost prevents large scale phenotyping as needed in breeding programs. Therefore, a calibration by means of Raman scattering spectrometry has been established in order to predict FA composition in rainbow trout Onchorhynchus mykiss adipose tissue. FA composition of visceral adipose tissue was analysed by both GC and Raman micro-spectrometry techniques on 268 individuals fed with three different feeds, which have different FA compositions. Among the possible regression methods, the ridge regression method, was found to be efficient to establish calibration models from the GC and spectral data. The best cross-validated R2 values were obtained for total PUFAs, omega-6 (Ω-6) and omega-3 (Ω-3) PUFA (0.79, 0.83 and 0.66, respectively). For individual Ω-3 PUFAs, α-linolenic acid (ALA, C18:3), eicosapentaenoic acid (EPA, C20:5) and docosahexenoic acid (DHA, C22:6) were found to have the best R2 values (0.82, 0.76 and 0.81, respectively). This study demonstrates that Raman spectroscopy could be used to obtain good correlation coefficients on adipocytes allowing to predict PUFAs, and calibration models can be used to predict PUFAs contents for large scale and high throughput phenotyping in rainbow trout.

Graphical abstract

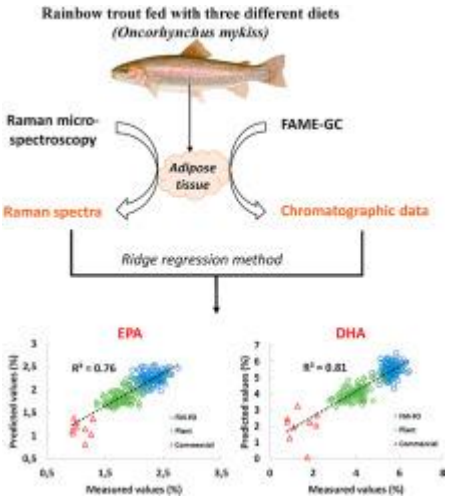

Highlights

► Fatty acids composition was predicted in rainbow trout *Onchorhynchus mykiss.* ► Three different feeds allowed to obtain different fatty acids composition. ► Raman spectroscopy was used to analyze adipose tissues from rainbow trout. ► Ω-3 eicosapentaenoic and docosahexenoic fatty acids have great R^2 values. ► Calibration models can be used for large scale and high throughput phenotyping.

Keywords : Raman spectroscopy, fatty acids, rainbow trout, adipocytes, calibration model, ridge regression method

INTRODUCTION

Nowadays, it is well known that fatty acids (FAs) play a major role as sources of metabolic energy for growth and physiological functions in body. It explains the increased attention paid in recent decades to the FA composition in human and animal nutrition. Among FAs, omega-3 (Ω-3) poly-unsaturated FAs (PUFAs), have a positive effect on the development and maintenance of vital physiological processes such as brain function, immune and inflammatory responses as well as a protective effect against cardiovascular diseases. Conversely, a higher content of Ω -6 PUFA coupled with a deficit of Ω -3 promotes obesity or cardiovascular

diseases [1, 2]. The European Food Safety Authority has confirmed that nutritional intake of Ω-3 PUFA (eicosapentaenoic acid (EPA, C20:5) and docosahexaenoic acid (DHA, C22:6)) have health benefits [2]. While saturated FAs (SFAs) and mono-unsaturated FAs (MUFAs) are synthesized in the body, PUFAs of the Ω-6 and Ω-3 families, at least linoleic acid (LA – C18:2 – Ω-6) and α-linolenic (ALA – C18:3 – Ω-3) acid, must be provided by the diet. Indeed, LA and ALA are Ω-6 and Ω-3 precursors, respectively, and the endogenous biosynthesis pathway provides low yields of long chains PUFAs [3]. Thus, it is important that the nutritional intake in humans of Ω-3 and Ω-6 with an adequate ratio be promoted by an appropriate diet.

Among the food products, fish represent the main source in terms of essential nutrients such as PUFAs, particularly long chains PUFA Ω-3. In fish, their compositions and quantity are influenced mostly by feed composition and feeding practices, environmental factors and genetic determinisms [3, 4]. It is well known that the feed influence greatly the FA composition of fish fillet, and therefore its nutritional value [3, 5]. Besides, it has also been proved that muscle FA composition is partly controlled by genetic determinism [6]. To improve FA composition by genetic selection it is necessary to estimate genetic parameters of FA composition in order to optimize the design of breeding programs PUFAs bioconversion and/or retention abilities. Among the most important farmed salmonid species reared worldwide, the production of rainbow trout reaches 848 000 tons per year [7]. Its flesh is well known for its healthy composition in PUFAs and for its lower lipid content than Atlantic salmon. If PUFAs composition in farmed fishes is mostly determined by the feed composition, there is no publication reported on estimation of genetic parameters of FAs composition in rainbow trout. This estimation and/or investment in genetic selection will require the phenotyping, *i.e.* the measurement of FA compositions on a large number of individuals and candidates. This is necessary to rank candidates according to their estimated breeding value. This phenotyping will require rapid affordable methods that can be applied to a large number of individuals.

Several conventional techniques with lipid extraction [8] and gas chromatography (GC) [9-11] are usually used to perform FAs analyses. However, these techniques have several disadvantages such as the use of solvents, the preparation time of samples before analysis and their high cost, so, they are not applicable at a large scale. For~~,~~ the development of breeding programs to improve FAs composition, it is necessary to use more affordable technologies than the FAME-GC as reference method.

Among different techniques, vibrational spectroscopic techniques like near-infrared (NIR) and mid-infrared Fourier Transform Infrared (MIR FTIR) spectroscopy have been employed in several studies to predict FA composition [12-15]. Another technique, the Raman spectroscopy, is also a powerful analytical method applicable for differentiation and identification of molecules of biological interest. Raman spectroscopy is also of significant interest because of its low sensitivity to the water content of the samples, which affects much more severely other vibrational spectroscopy techniques such as NIR and MIR FTIR spectroscopy. As an example, concentrations of EPA, DHA and total Ω-3 FAs have been well predicted in fish oils, by using infrared and Raman techniques [14]. Besides its ability to be used *in vivo*, Raman spectral bands are thinner than those obtained by NIR spectroscopy, allowing more accurate band assignments to molecular vibrational modes. To the best of our knowledge, no studies were realized yet on the prediction of different FA classes and/or individual FAs in fishes using Raman spectroscopy.

In this work, we present a calibration model using a statistical regression analysis by combining Raman spectroscopy and GC data to allow the prediction of FAs in the visceral adipose tissue of rainbow trout (*Oncorhynchus mykiss*). The objective of this study is to determine the FAs composition of these adipose tissues of rainbow trout in order to evaluate the efficiency of Raman spectroscopy as a routine FAs analysis method needed for breeding programs.

MATERIALS & METHODS

1. Raman calibration sampling

The Raman calibration used 259 rainbow trout collected at the INRAE experimental facility of PEIMA (Sizun, France). Trout from PEIMA belonged to the same batch and were fed with a commercial feed until they reached an average weight of 600 g.

They were then splitted in two groups: one group (N=129) continue to be fed with a commercial feed containing fish meal and fish oil (BioExtra F7, Le Gouessant), the second group (N=130) was fed with a plant-based feed devoid of long chains PUFA Ω-3 (INRAE, Pisciculture de Donzacq)) during 4 months. These two feeds differed in their FA composition and they were used to induce changes in the fatty acid profiles of fish tissues. Fish were euthanized and visceral fat samples were collected from the same "front" lobe of visceral adipose tissues, placed in a coded aluminium foil (10 g) or in cryotubes (2 g), for GC or Raman measurements, respectively, and were preserved in liquid nitrogen until further analyses. Nine additional samples from rainbow trout, reared under commercial conditions (Aqualande group, Viviers de la Hountine, Belin Béliet, France) and fed with a commercial feed (Viva Pro 7F, Aqualia), were also analysed.

2. Gas chromatography (GC) analysis– reference analytical method

The fatty acid composition was determined for each calibration sample after lipid extraction by cold biphasic method, methylation of FAs and analysis of the fatty acid methyl esters by GC reference method (Eurofins Analytics, Nantes, France). The FAs proportion is defined by the relative concentrations of the different FAs present in sample and generally compared to each other by considering the major families of SFAs, MUFAs and PUFAs. The proportion of these latter, as well as Ω-3 and Ω-6 FAs (total and individual), are calculated. The detection limit is

126 estimated at 0.05 % of the total fatty acids and the measurement uncertainty (MU) is calculated
127 from the following equation, provided by EuroFins:

128 $$MU = 0.25 + \sqrt{(0.1 * \%FA)}$$

129 where %FA correspond to the calculated proportion of FAs expressed in percent of total FAs.
130 Major FA group correspond to SFAs, MUFAs, PUFAs, total Omega-3 and total Omega-6.
131 SFAs were the sum of C14:0, C15:0, C16:0, C17:0, C18:0 and C20:0. MUFAs were the sum
132 of C16:1, C18:1, C20:1 and C22:1. PUFAs were the sum of C16:2, C16:3, C16:4, C18:2, C18:3,
133 C20:2, C20:3, C20:4, C18:3, C18:4, C20:3, C20:4, C20:5 and C22:6. Total Ω-6 FAs were the
134 sum of 18:2, 18:3, 20:2, 20:3 and 20:4. Total Ω-3 FAs were the sum of 18:3, 18:4, 20:5, 22:5
135 and 22:6.

136 **3. Raman instrumentation and spectra acquisition parameters**

137 A small piece of frozen sample (50-100 mg) was placed in a glass cup, cut rapidly with a scalpel
138 then rise at room temperature before placing under the microscope. The visceral adipose tissue
139 was selected as the first approach of our studies because adipocyte cells can be directly targeted
140 by the laser beam through a microscope objective in order to determine the FA composition.
141 The adipocyte cells were also studied to avoid bias, interference from unknown sources or lower
142 precision potentially associated with the cellular organization of the muscle in the fillet (mainly
143 connective tissues, muscle fibres or blood vessels).
144 Raman spectra were collected with a micro-spectrometer LabRAM HR800 (Horiba Scientific),
145 with a selected 600 g/mm grating suitable for the spectral resolution required for this study and
146 a charge-coupled device (CCD) detector cooled at -75°C. The Raman system was equipped
147 with three laser sources: 532 nm, 633 nm and 785 nm. In a first approach, although the
148 excitation laser at 785 nm should show less fluorescence for biological samples, all wavelengths
149 were tested and two spectral ranges were acquired through a 10x objective: 550 to 1800 cm^{-1}

and 2610 to 3100 cm^{-1} with two accumulations with acquisition times of 20 s and 30 s and, respectively.

4. Raman spectral treatment and statistical analysis by ridge regression.

The first preliminary step consists to average replica spectra of reference samples. Then, a baseline fitted by rubberband method to each spectrum was subtracted of all spectra to remove the contribution of fluorescence and background noise from the spectra. The standard normal variate transformation, which is basically a signal intensity normalisation, was applied on the baseline-subtracted Raman spectra to eliminate variations in the general intensity.

Pre-processed Raman spectra covering two different frequency regions (550-1800 cm^{-1} and 2610-3100 cm^{-1}) were used to develop multivariate linear regression models based on partial least squares (PLS) [16] and *ridge* regression methods [17]. Briefly, PLS constructs a set of linear combinations of the inputs for regression, while the ridge regression also allows to apply penalties on the least important features, *i.e.*, the ones that contribute little to the final result. All treatments are realized with R using packages for the baseline [18], the PLS [16] and the ridge regression method (*glmnet* package) [19]. Both methods are especially designed to estimate linear prediction scores when the number of predicting variables, here the Raman spectrum values at each wavenumber, exceeds the training sample size. The ridge method introduces a shrinkage parameter whose optimization aims at finding the best compromise between prediction bias and variance. The R package glmnet implements such an optimization method.

A 10-fold cross-validation procedure was used to compare the prediction performance of each model by the squared correlation between predicted and observed responses (cross-validated R^2) and the root mean square error of prediction (RMSEP).

Regarding their prediction performance, ridge regression showed the best results and was finally selected to develop the calibration model.

RESULTS AND DISCUSSION

1. Excitation wavelength selection and spectral assignment of vibrational bands

A wide range of factors influences the intensity of Raman spectra of biological samples including instrumental parameter as laser intensity, wavelength, and acquisition time. In this study, three wavelengths were tested (532nm, 633nm and 785nm) on the sample in order to select the most suitable for measuring lipids in adipose tissues of rainbow trout and to obtain robust multivariate calibration models. Figure 1 shows the representative spectra of visceral adipose tissue acquired with the three different wavelengths. In order to be comparable, the spectra were just normalized by the acquisition time. The most characteristic features of Raman spectra of lipids related to hydrocarbon chain were observed in the three spectra, notably C=C bonds or CH_2 group vibration at ~ 1650 cm^{-1} and ~1450 cm^{-1}, respectively [20, 21]. This strong lipid fingerprint seems coherent with the Raman spectrum of a biological tissue containing a large amount of lipids and associated molecules (FAs, triglycerides, etc) as adipose tissues. As expected, this fluorescence contribution decreased when the 633 and 785 nm excitation wavelengths were used. Nevertheless, the Raman intensity of high wavenumber vibrations was dramatically reduced at 785 nm. Indeed, when considering the near-infrared 785 nm excitation, CCD efficiency radically decreased for such high wavenumbers. Considering the above-mentioned effects, the 785 nm wavelength was selected for the present study. Using this wavelength will therefore allow to acquire informative spectral information from visceral adipose tissues of rainbow trout.

The stability and homogeneity of the samples were tested by recording the Raman spectrum at the same position at regular time intervals (of about 5') for 30' (physical replicas) or by measuring the Raman spectrum at different positions in the sample (biological replicas). No significant signal evolution was observed during the 30' acquisition of the physical replicas. In

the case of the biological replicas, the visceral fat front lobe was separated into five samples, all measured independently. The similarity of the spectra obtained confirmed the high homogeneity of the visceral tissue. As in the case of physical replicas, the variations in intensity observed between 600 and 1200 cm^{-1} can be explained by a change in background noise that may be due to a variation in the biological environment such as presence of traces of blood and/or pieces of cell membranes.

The numbers in Figure 2 correspond to the Raman spectral band assignments provided in Table 1 based on literature [21]. Among the major and characteristic spectral vibrations, the bands 1 and 2, at 601 and 727 cm^{-1}, respectively, could be attributed to particular vibration mode of phospholipids and trimethylamine, respectively, thus they are characteristic of lipidic cellular membrane. The band 16 at 1748 cm^{-1} corresponded to (C=O) stretching vibration of ester functional groups from lipids and FAs and the band 21 at 3013 cm^{-1} to (=C-H) stretching of unsaturated fatty acids. Note that the assignment of band 15 at ~1650 cm^{-1} corresponded to (C=C) stretching mode of unsaturation in *cis* conformation, *trans* conformation induced a band shift at 1670 cm^{-1}. In the present study, no significant signal was observed at 1670 cm^{-1}, showing a clear majority of the *cis* conformation of fatty acid unsaturation in visceral adipose tissue of rainbow trout.

2. Fatty acid composition of rainbow trout feeds

FAME-GC measurements were realized to determine the FA composition of the different feeds used in this study: the feed containing fish meal and fish oil (FM-FO feed) and the plant-based feed fed by the trout from PEIMA, and the commercial feed fed by the trout from Aqualande (Table 2). The predominant FAs in all fish feeds were C16:0, C18:1, LA (18:2 Ω-6), ALA (C18:3 Ω-3), EPA (C20:5 Ω-3) and DHA (C22:6 Ω-3) fatty acids. Feeds contained different proportions of SFAs: 27.31%, 21.71%, and 13.83%, for FM-FO, plant, and commercial feeds, respectively. Differences between feeds were observed in the proportions of

MUFAs: 31.46%, 40.26%, and 56.24%, for FM-FO, plant, commercial feeds, respectively. These differences were mainly due to 18:1.

The proportion of Ω-6 fatty acids in the FM-FO feed was 28.77% and this value was higher than in the plant feed (19.25%), and commercial feed (19.33%). Differences were found between all three feeds in the content of Ω-3 fatty acids. The proportion of Ω-3 fatty acids was highest in the plant-based (18.73%) which contain only ALA, followed by 10.24%, in the FM-FO feed, and 9.82% in the commercial feed. The plant-based feed was totally devoid of EPA and DHA, whereas the proportions of EPA in the feeds were 2.21% (FM-FO feed) and 0.95% (commercial feed), and those of DHA were 1.99% (FM-FO feed), and 1.15% (commercial feed). These differences in FA composition reflected the nature of the ingredients incorporated in the feeds, in particular the proportions of FM-FO, the main sources of EPA and DHA, versus the proportions of vegetable ingredients, rich in 18:1, LA and ALA. It is now well known that the FA composition of fish tissues reflected in a large manner that of the feeds [22-24]. So, we expected in this study to have different FA profiles in perivisceral adipose tissue, the main lipid storage site in rainbow trout, that allow to predict them by Raman spectroscopy after calibration.

3. Prediction of fatty acid composition from visceral adipose tissue of rainbow trout

Table 3 presented the data determined by FAME-GC analysis on the FA composition of adipose tissue of the three groups of rainbow trout fed with the different feeds (FM-FO, plant-based, commercial). Adipose tissue of fish fed with the commercial feed contains more SFAs and MUFAs compared to the other two groups (FM-FO and plant-based feeds). The most important SFAs and MUFAs in adipose tissue were the FAs 16:0 and 18:1 in accordance with the proportions of these FAs in the feeds. These data are consistent with previously published data on FA composition of adipose tissue in rainbow trout [24, 25].

LA is the main PUFA Ω-6 present in adipose tissue, reflecting the abundance of this FA in the three feeds. However, the proportion of LA in adipose tissue of trout fed with the FM-FO

feed was 20.86%, which is lower than the proportion directly found in the feed (28.57%). This seems to indicate that LA is more metabolized in trout fed with the FM-FO feeds, confirming previous observations that LA is readily oxidized when present at high concentrations [3, 23]. For Ω-3 FAs, the higher proportion of ALA (6.29%) was found in fish fed with plant-based feed, which is the richest in ALA (18.73%) whereas the fish fed with the FM-FO feeds had the highest proportions of EPA and DHA compared to the other two groups. It is interesting to note that DHA is present at 3.94% in visceral fat of trout fed with the plant-based feed, despite the absence of this FA in the feeds. As these fish were previously fed with a commercial feed containing FM and FO, this may be due to a selective retention of DHA and/or a biosynthesis from the precursor ALA [3, 23, 26]. Overall, these data confirm that dietary FA composition is minored in the fish's tissues; even the difference in the percentage of fatty acids between feeds is greater than the difference observed in tissues of fish fed these feeds [27-29]. Besides dietary effects, the incorporation of fatty acids into fish tissue is under various metabolic influences, such as preferential incorporation, β-oxidation, lipogenic activity or fatty acid elongation and desaturation processes [3, 23]. These metabolic influences can explain the individual variability observed in FA composition and highlight the interest of a method for predicting FA composition for breeding programs.

The coefficient of variation (CV) was also calculated for each FAs of interest, as displayed in Table 3. It can be observed that the CVs calculated for the SFA in rainbow trout are 0.82, 3.63, and 5.51%, for the FM-FO, plant- and commercial-based feeds, respectively. Thus, the dispersion is very important for visceral adipose tissues from rainbow trout fed with the commercial-based feed, compared to those from fed with FM-FO feed. This difference in the distribution of values is clearly illustrated by the Figure 3.A, and could be explained by the individual variability due to various metabolic influences, as mentioned above. The same observation can be made for PUFAs: 0.55, 2.92, and 5.20%, for the FM-FO, plant- and

commercial-based feeds, respectively (Figure 3.C); and total Ω-3: 0.98, 5.05, and 11.27%, for the FM-FO, plant- and commercial-based feeds, respectively (Figure 3.D). For individual Ω-3 FAs, the CVs were calculated for ALA: 4.51, 9.38, and 4.47%, for the FM-FO, plant- and commercial-based feeds, respectively (Figure 4.A); for EPA: 3.49, 10.67, and 12.96%, for the FM-FO, plant- and commercial-based feeds, respectively (Figure 4.B); and for DHA: 2.84, 12.43, and 39.16%, for the FM-FO, plant- and commercial-based feeds, respectively (Figure 4.D). Surprisingly, an important dispersion is observed for DHA from rainbow trout fed with commercial-based feed. It could be hypothesized that all individuals could not metabolize in an equal manner commercial feed in order to obtain long-chain PUFAs Ω-3, such as DHA, explaining thus the lower composition compared to those obtained with FM-FO and plant-based feeds. To add more weight to this hypothesis, the CVs were calculated for individual Ω-6 FAs. It was obtained for LA: 1.87, 3.17, and 4.17%, for the FM-FO, plant- and commercial-based feeds, respectively (Figure 5.A); for ARA: 16.28, 13.89, and 23.53%, for the FM-FO, plant- and commercial-based feeds, respectively (Figure 5.C). It can be observed a more important dispersion for C20:4 from rainbow trout fed with commercial-based feed. Thus, the metabolization of the commercial feed by some individuals could be less effective for obtaining long-chain PUFAs Ω-6, compared to other feeds.

The whole set of data used for calibration with mean values and standard deviations regarding major FAs group and 18 individual FAs are given in Table 4. A large variability was present in major FAs groups as demonstrated by the broad ranges and relative standard deviation observed. This variability was expected since the fish were fed with feeds differing in their FA composition. As shown in Table 4, the most abundant FAs identified are: 16:0, 18:1 and 18:2 Ω-6 (LA: linoleic acid) with an abundance upper 10%; and 18:3 Ω-3 (ALA: alpha-linolenic acid), 20:1, 20:5 Ω-3 (EPA), and 22:6 Ω-3 (DHA) with an abundance between 1 to 10 %. FAs, which represented less than 1% of the total FA content, would not have signals

identifiable by Raman spectroscopy [30]. In our study, the FAs such as 15:0, 17:0, 20:0, 18:3 Ω-6, 20:2 Ω-6, 20:3 Ω-6, 20:4 Ω-6, 18:4 Ω-3 and 22:5 Ω-3 are concerned due to their low abundance in visceral fat.

The first reason to choose visceral adipose tissue is that this tissue is the only available in sufficient quantity in order to perform GC analyses on individual fish. This choice was also planned to simplify interpretation of Raman spectra as visceral adipose tissue is mostly composed of adipocytes to avoid contamination with, for example, the presence of muscle proteins or blood in the flesh as in the muscle. The visceral adipose tissue presents the advantages to be homogeneous and to not contain any or very few fluorescent molecules, compared to the muscle tissue. Raman spectroscopy being a technique sensitive to the fluorescence, masking usually the Raman signal. Raman measurements on a minced standard portion of the muscle (known as Norwegian Quality Cut) as done by Difford et al., 2021 to estimate total lipid content, implies in practice an additional step of mincing that was not preferred for future applications as in breeding programs [31]. The Raman characterisation of fat in the adipocytes from the visceral adipose tissue was also preferred because viscera seem to be preferentially a lipid deposition site according to other studies [32, 33]. Hixxon et al. showed that the lipid composition of the visceral adipose tissue most reflected that of the feed. Indeed, most of the stored lipid came from the accumulation of lipids from the feed of rainbow trout [34]. However recent advances have also reported that visceral or subcutaneous adipocytes in Atlantic salmon may have different physiological functions (energy stocking and immunology vs energy metabolism) and potentially different FA compositions. Thus, in tissues with limited amounts of adipocytes (*e.g.* subcutaneous, dorsal fat or muscle myosepta), our study may have a particular interest in the prediction of individual FAs [35].

Summary statistics for each major FA group and for each individual FA are displayed in Table 4. Prediction performance using ridge regression is assessed by cross-validated R^2 and

RMSEP. Also, correlation plots for predicted values *vs* measured values on visceral fat are shown in Figures 3, 4, and 5, in order to illustrate the prediction performance of each trait. SFA group showed a weaker prediction performance (R^2=0.42). Yet, one of the most abundant SFAs, 16:0 (12.73%), presented a high R^2 value of 0.71. Although this FA represented about 66% of the total SFAs, its good prediction performance is not enough to influence the overall prediction of the total SFAs. Other less abundant SFAs, 14:0 and 18:0, represented about 10.6% and 17.3% of the total SFAs, respectively. While 14:0 showed a good R^2 value of 0.70, the 18:0 displayed a poor R^2 value of 0.44. It can be hypothesized that 18:0 could be mostly responsible to the decrease of the prediction performance of the total SFAs. However, Behre et al., studying fatty acids prediction in pork adipose tissues, obtained better R^2 results for the same SFAs: 14 :0 (1.1%), 16 :0 (22.4%) and 18 :0 (12.9%), for R^2 values of 0.67, 0.89 and 0.72, respectively [36]. Other studies suggested that vibrations of SFAs, depending on the polymorphic form of these latter, could be split over multiple spectral regions [37, 38]. This could also explain the poor prediction performance for SFAs. Good prediction performance was observed for MUFAs (R^2=0.75) and PUFAs (R^2=0.79). Indeed, the more carbon double bonds will be present in the FA chains of MUFAs and PUFAs, the more the Raman signal of these spectral vibrations, such as at 1267 cm^{-1} (=C-H deformation) and 1658 cm^{-1} (C=C stretching) will increase. Thus, having a high prediction performance for the MUFAs and PUFAs concentrations could indicate that it would be an increase of the spectral vibrations' intensities within the Raman spectra [39]. Within the PUFAs, the total Ω-3 and total Ω-6 groups were distinguished and R^2 were obtained. The total Ω-6 FA group shows a R^2 of 0.83, whereas the performance of total Ω-3 FA group was weaker (R^2=0.66). R^2 were also determined for individual Ω-3 and Ω-6 FA. Poor to intermediate prediction performances were obtained for 20:3, 20:2, and 18:3 : R^2 values were 0.02, 0.04, and 0.46, respectively. These Ω-6 FAs could explain their low R^2 by their mean weight of the percentage being < 1%. Thus, considering limited predicting individual Ω-6 FAs

to predict total Ω-6 could explain the decrease of the overall prediction performance of this FA group. The same hypothesis could be verified with the individual Ω-3 FAs. R^2 values of 18:4 and 22:5 were 0.04 and 0.44, respectively. These two Ω-3 FAs have a poor to intermediate prediction performance certainly due to their mean weight of the percentage being < 1%, and would not have signals identifiable by Raman spectroscopy [30]. Thus, taking into account these two individual FAs could explain the decrease of the overall prediction performance of the Ω-3 FA group. More precisely, the impact of the co-variance of individual FAs on the R^2 values of FA groups may be hypothesized. A recent study investigates the prediction of individual FAs and total FA depending on variation of the iodine value in pork backfat, which were fed with different dietary fat sources and levels. Good correlations were obtained (R^2 = 0.78–0.90) [36]. However, they report that the individual FAs predictions are indirect and strongly depend on co-variance with the relative FAs composition. Based on this observation, our results seem to show that low R^2 values of individual FAs could influence the prediction performance of FA groups.

It is noted that moderate to very good R^2 values were found for the Ω-6 LA and arachidonic acid, and the Ω-3 ALA, EPA, DHA: 0.84, 0.61, 0.82, 0.76, and 0.81, respectively. These FAs displaying great prediction performance are usually well predicted in other studies [14, 18]. For instance, high correlation coefficients (0.85-0.97) were previously obtained in commercial Ω-3 PUFA oil supplements capsules enriched in FAs with much higher EPA (24.1 %-27.7%) and DHA (18.6%-20.6%) concentrations [18]. Another study showed very good correlation values of 0.97 and 0.9, for EPA and DHA respectively [14]. The much lower concentration in EPA and DHA in visceral fat compared to concentrated fish oil may explain the lower prediction performance obtained in this study (0.76, and 0.81). However, our correlation coefficients are sufficiently high to enable high throughput estimation of FAs compositions in adipocyte cells. As handheld Raman probes have already been used to estimate lipid composition of fish [40,

41] and fish oils [42], it will be interesting to associate this nondestructive technology with minimally invasive biopsy in order to phenotype live or dead fishes for diverse aquaculture or conservation applications (nutrition, reproduction, genetic improvement).

CONCLUSION

Our study was based on calibration of FA composition and prediction in visceral adipose tissue as a first step of investigation and development for application of Raman spectroscopy in fish and aquaculture breeding. The effective of individuals considered in the calibration will gain to be extended for more broad and accurate predictions taking into account different FA compositions, fish size and genotypes. The adipocyte cell was easily targeted by the laser ray with our Raman apparatus equipped with a microscope. Transfer of the results to other Raman device as portable device will need caution before extensive application. Our results also open the way for fine surveys of adipocyte cell composition depending on tissues, biological factors (age, sex, genotypes, polyploidy, species) or zootechnical practices (feeding strategy, feed composition, rearing temperature, fish density) in decreasing potentially cost and time of measurements. It also opens the way for *in vivo* measurement and repeated measurements based on tissue coring on live animals in respecting welfare international recommendations and regulations. Transfer of the results to other kind of tissues or aquaculture species may need careful validation. Prediction performances are variable according to the FAs and/or groups or sums or ratios investigated. If for quality control procedures, high performances of prediction are required, the benefit/cost ratio needs estimation for the different predicted FAs. Thus, this methodology shows that moderate to good correlation coefficients can be obtained to predict PUFAs, and calibration models can be used to predict PUFAs contents for large scale and high throughput phenotyping.

ACKNOWLEDGEMENTS

This study was partly funded by The European Maritime and Fisheries Fund and FranceAgrimer (Omega-Truite project, n° PFEA47 0017 FA 1000008). The authors thank the INRAE's experimental facilities (PEIMA) for fish rearing and their technical assistance for adipose tissue sampling.

ETHICS STATEMENT

This study was conducted in accordance with EU Directive 2010-63-EU on the protection of animals used for scientific purposes. The fish farmed at the INRAE experimental station of PEIMA (UE 0937) agreed under N° C29 -277 -02 were reared according to normal husbandry practices, and were not subjected to practices likely to cause pain, suffering, distress or lasting harm equivalent to, or higher than, that caused by the introduction of a needle in accordance with good veterinary practice. As such, the experiment did not require approval by an Ethics Committee, in accordance with Article 2.5 of the EU Directive 2010-63-EU.

REFERENCES

[1] P.C. Calder, P. Yaqoob. Omega-3 polyunsaturated fatty acids and human health outcomes. *Biofactors*, 35(2009), 266-72.

[2] C. Ruxton, S. Reed, M. Simpson, K. Millington. The health benefits of omega-3 polyunsaturated fatty acids: a review of the evidence. *J Hum Nutr Diet*., 20 (2007), 275-85.

[3] D.R. Tocher DR, Omega-3 long-chain polyunsaturated fatty acids and aquaculture in perspective, *Aquaculture*, 449 (2015), 94-107.

[4] S.S. Horn, B. Ruyter, T.H.E. Meuwissen, B. Hillestad, A.K. Sonesson, Genetic effects of fatty acid composition in muscle of Atlantic salmon, *Genet. Sel. Evol.* 50 (2018) 1–12.

[5] G.M. Turchini, D.S. Francis, R.S.J. Keast, A.J. Sinclair. Transforming salmonid aquaculture from a consumer to a producer of long chain omega-3 fatty acids. *Food Chemistry*., 124 (2011), 609-614.

[6] J.G. Bell, J. Pratoomyot, F. Strachan, R.J. Henderson, R. Fontanillas, A. Hebard, D.R. Guy, D. Hunter, D.R. Tocher, Growth, flesh adiposity and fatty acid composition of Atlantic salmon (*Salmo salar*) families with contrasting flesh adiposity: Effects of replacement of dietary fish oil with vegetable oils, *Aquaculture*., 306 (2010), 225–232.

[7] Food and Agriculture Organization (FAO), 2020, The State of World Fisheries and Aquaculture 2020, Sustainability in action, Rome.

[8] C. Breil, M. Abert Vian, T. Zemb, W. Kunz, F. Chemat. "Bligh and Dyer" and Folch methods for solid–liquid–liquid extraction of lipids from microorganisms: Comprehension of solvatation mechanisms and towards substitution with alternative solvents. *Int. J. Mol. Sci*. 18 (2017), 1–21.

[9] L.D. Roberts, G. McCombie, C.M. Titman, J.L. Griffin. A matter of fat: an introduction to lipidomic profiling methods. *J Chromatogr B.*, 871 (2008), 174e81.

[10] J. Ecker, M. Scherer, G. Schmitz, G. Liebisch. A rapid GC-MS method for quantification of positional and geometric isomers of fatty acid methyl esters. *J Chromatogr B.*, 897(2012), 98e104.

[11] E. Indarti, M.I.A. Majid, R. Hashim, A. Chong. Direct FAME synthesis for rapid total lipid analysis from fish oil and cod liver oil, *J. Food Comp. Anal.*, 18 (2005), 161-170.

444 [12] N. Prieto, M.E. Dugan, O. López-Campos, T.A. McAllister, J.L. Aalhus, B. Uttaro. Near
445 infrared reflectance spectroscopy predicts the content of polyunsaturated fatty acids and
446 biohydrogenation products in the subcutaneous fat of beef cows fed flaxseed. *Meat Sci*.
447 90(2012), 43-51.

448 [13] C. Piotrowski, R. Garcia, A. Garrido-Varo, D. Pérez-Marín, C. Riccioli, T. Fearn. The
449 potential of portable near infrared spectroscopy for assuring quality and authenticity in the food
450 chain, using Iberian hams as an example. *Animal*. 13(2019), 3018-3021.

451 [14] M.Y. Bekhit, B. Grung, S.A. Mjøs. Determination of omega-3 fatty acids in fish oil
452 supplements using vibrational spectroscopy and chemometric methods, *Appl. Spectrosc*. 68
453 (2014), 1190–1200.

454 [15] E. Giese, O. Winkelmann, S. Rohn, J. Fritsche. Determining quality parameters of fish oils
455 by means of 1H nuclear magnetic resonance, mid-infrared, and near-infrared spectroscopy in
456 combination with multivariate statistics. *Food Res Int*. 106(2018), 116-128.

457 [16] B-H. Mevik, R. Wehrens, K.H. Liland, PLS: Partial Least Squares and Principal
458 Component Regression, 2020, R package version 2.7-3. https://CRAN.R-
459 project.org/package=pls

460 [17] Z. Chen, T. Wu, C. Xiang, X. Xu, X. Tian, Rapid identification of rainbow trout
461 adulteration in Atlantic salmon by Raman spectroscopy combined with machine learning,
462 *Molecules*. 24 (2019), 2851

463 [18] K.H. Liland, T. Almøy, B-H. Mevik. Optimal Choice of Baseline Correction for
464 Multivariate Calibration of Spectra. *Appl. Spectrosc*. 64(2010), 1007-1016.

[19] J. Friedman, T. Hastie, R. Tibshirani, Regularization Paths for Generalized Linear Models via Coordinate Descent, *J. Stat. Soft.* 33(2010), 1-22.

[20] Z. Movasaghi, S. Rehman, I.U. Rehman, Raman Spectroscopy of Biological Tissues. *Appl. Spectrosc. Rev*., 42 (2007), 493–541.

[21] K. Czamara, K. Majzner, M.Z. Pacia, K. Kochan, A. Kaczor, M. Baranska. Raman Spectroscopy of Lipids: A Review: Raman Spectroscopy of Lipids. *J. Raman Spectrosc*., 46(2015), 4–20.

[22] M.J. Caballero, A. Obach, G. Rosenlund, D. Montero, M. Gisvold, M.S. Izquierdo. Impact of different dietary lipid sources on growth, lipid digestibility, tissue fatty acid composition and histology of rainbow trout, *Oncorhynchus mykiss*. *Aquaculture*, 214(2002), 253–271.

[23] J. Fonseca-Madrigal, J.G. Bell, D.R. Tocher. Nutritional and environmental regulation of the synthesis of highly unsaturated fatty acids and of fatty-acid oxidation in Atlantic salmon (*Salmo salar L.*) enterocytes and hepatocytes. *Fish Physiol. Biochem*. 32(2006), 317–328.

[24] G.M. Turchini, B.E. Torstensen, W.K. Ng.,. Fish oil replacement in finfish nutrition. *Rev. Aquacult*., 1(2009), 10–57.

[25] A. Kiessling, J. Pickova, L. Johansson, T. Åsgård, T. Storebakken, K.H. Kiessling. Changes in Fatty Acid Composition in Muscle and Adipose Tissue of Farmed Rainbow Trout (*Oncorhynchus Mykiss*) in Relation to Ration and Age. *Food Chem*. 73(2001), 271–284.

[26] H. İbrahim Haliloğlu, A. Bayır, A. Necdet Sirkecioğlu, N. Mevlüt Aras, M. Atamanalp. Comparison of Fatty Acid Composition in Some Tissues of Rainbow Trout (*Oncorhynchus Mykiss*) Living in Seawater and Freshwater. *Food Chem*. 86 (2004), 55–59.

[27] V. Lazzarotto, F. Médale, L. Larroquet, G. Corraze. Long-term dietary replacement of

fishmeal and fish oil in feeds for rainbow trout (*Oncorhynchus mykiss*): Effects on growth, whole body fatty acids and intestinal and hepatic gene expression. *PLoS One*, 13(2018), 1–25.

[28] D. Trbovi, D. Vrani, J. Djinovic-stojanovi, D. Spiri, J. Babi, R. Petronijevi, A. Spiri. Fatty acid profile in rainbow trout (*Oncorhynhus Mykiss*) as influenced by diet, *Biotech. Anim. Husb.*, 28(2012), 563–573.

[29] N. Richard, S. Kaushik, L. Larroquet, S. Panserat, G. Corraze. Replacing Dietary Fish Oil by Vegetable Oils Has Little Effect on Lipogenesis, Lipid Transport and Tissue Lipid Uptake in Rainbow Trout (*Oncorhynchus Mykiss*). *Br. J. Nutr.* 96(2006), 299–309.

[30] J.R. Beattie, S.E.J. Bell, C. Borgaard, A. Fearon, B.W. Moss, Prediction of adipose tissue composition using Raman spectroscopy: Average properties and individual fatty acids, *Lipids*. 41 (2006), 287–294.

[31] G.F. Difford, S.S. Horn, K.R. Dankel, B. Ruyter, B.S. Dagnachew, B. Hillestad, A.K. Sonesson, N.K. Afseth, The heritable landscape of near-infrared and Raman spectroscopic measurements to improve lipid content in Atlantic salmon fillets, *Genet. Sel. Evol*. 53 (2021), 1–11.

[32] G. Corraze, L. Larroquet, F. Médale. Alimentation et dépôts lipidiques chez la truite arc-en-ciel, effet de la température d'élevage. *INRAE Productions Animales*, 12 (1999), 249–256.

[33] A. Figueiredo-Silva, E. Rocha, J. Dias, P. Silva, P. Rema, E. Gomes, L.M.P. Valente, Partial replacement of fish oil by soybean oil on lipid distribution and liver histology in European sea bass (*Dicentrarchus labrax*) and rainbow trout (*Oncorhynchus mykiss*) juveniles, *Aquac. Nutr*. 11 (2005), 147–155.

[34] S.M. Hixson, C.C. Parrish, D.M. Anderson, Use of camelina oil to replace fish oil in feeds for farmed salmonids and atlantic cod, *Aquaculture*. 431 (2014), 44–52.

[35] M. Bou, X. Wang, M. Todorčević, T.K.K. Østbye, J. Torgersen, B. Ruyter, Lipid deposition and mobilisation in atlantic salmon adipocytes, Int. J. Mol. Sci. 21 (2020), 2332-2351.

[36] D.T. Berhe, C.E. Eskildsen, R. Lametsch, M.S. Hviid, F. van den Berg, S.B. Engelsen, Prediction of total fatty acid parameters and individual fatty acids in pork backfat using Raman spectroscopy and chemometrics: Understanding the cage of covariance between highly correlated fat parameters, *Meat Sci.* 111 (2016), 18–26.

[37] S. Bresson, M. El Marssi, B. Khelifa, Conformational influences of the polymorphic forms on the CO and C-H stretching modes of five saturated monoacid triglycerides studied by Raman spectroscopy at various temperatures, *Vib. Spectrosc*. 40 (2006), 263–269.

[38] S.M. Fowler, H. Schmidt, E.H. Clayton, R. Van De Ven, P. Wynn, D.L. Hopkins, Predicting Fatty Acid Composition of Lamb Loin Using Raman Spectroscopy, *IComst*. (2014), 4–7.

[39] E.F. Olsen, E.O. Rukke, A. Flåtten, T. Isaksson, Quantitative determination of saturated-, monounsaturated- and polyunsaturated fatty acids in pork adipose tissue with non-destructive Raman spectroscopy, *Meat Sci*. 76 (2007), 628–634.

[40] N.K. Afseth, M. Bloomfield, J.P. Wold, P. Matousek, A novel approach for subsurface through-skin analysis of salmon using spatially offset raman spectroscopy (SORS), *Appl. Spectrosc*. 68 (2014), 255–262.

529 [41] J.D. Landry, P.J. Torley, E.W. Blanch. Detection of Biomarkers Relating to Quality and
530 Differentiation of Some Commercially Significant Whole Fish Using Spatially Off-Set Raman
531 Spectroscopy. *Molecules*. 25(2020), 3776.

532 [42] D.P. Killeen, A. Card, K.C. Gordon, N.B. Perry, First Use of Handheld Raman
533 Spectroscopy to Analyze Omega-3 Fatty Acids in Intact Fish Oil Capsules, *Appl. Spectrosc*. 74
534 (2020), 365–371.

535
536
537
538
539
540
541
542
543
544
545
546
547
548
549
550
551
552

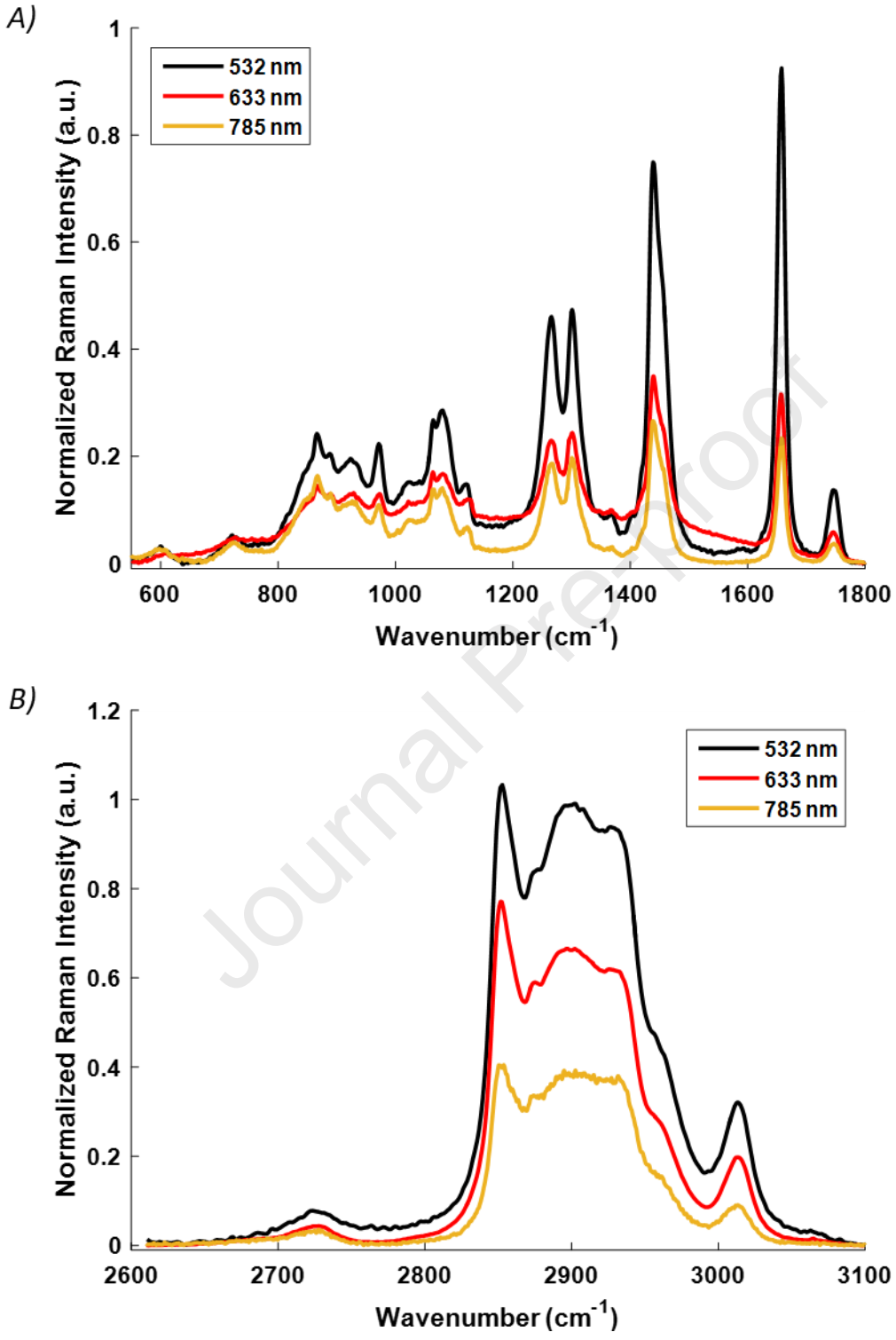

Fig. 1. Raman spectra of visceral adipose tissue from rainbow trout, acquired at different wavelengths: 532, 633 and 785 nm. (A) 550-1800 cm^{-1}, (B) 2600-3100 cm^{-1}

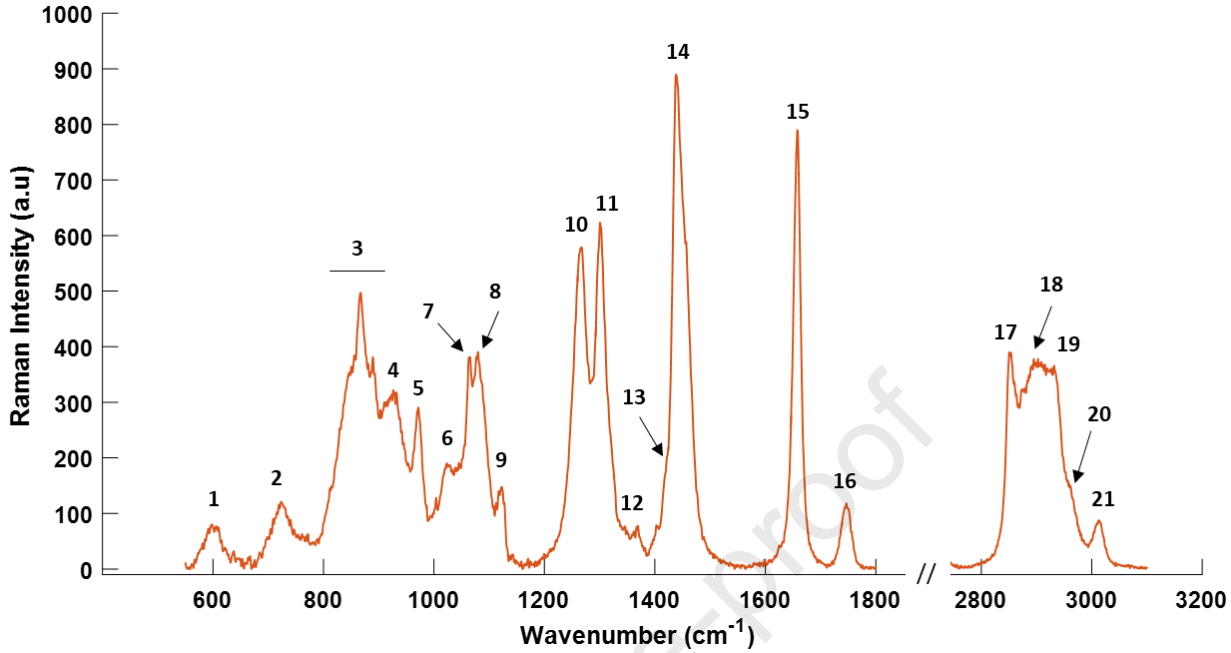

Fig. 2. Raman spectrum of visceral adipose tissue acquired at 785 nm.

574

575 **Table 1. Assignment of bands in the Raman spectra**

Number	Raman shift (cm^{-1})	Assignment
1	601	δ(C=O-C)
2	727	$\nu_s(N^+(CH_3)_3)$
3	845-889	ν(C-C)+ ν(C-O-C)
4	925	ν(CH)
5	972	ν(CH)
6	1025	ν(C-C)
7	1065	ν(C-C)
8	1080	ν(C-C)+ ν((PO^{4-})
9	1121	ν(C-C)
10	1267	δ(=C-H)
11	1303	$\delta_{as}(CH_2)$
12	1367	$\delta_{as}(CH_2)$
13	1420	$\delta_s(CH_2)$
14	1438	$\delta(CH_2/CH_3)$
15	1658	ν(C=C)
16	1748	ν(C=O)
17	2853	$\nu_s(=CH_2)$
18	2895	$\nu_{as}(=CH_2)$
19	2931	$\nu_s(=CH_3)$
20	2960	$\nu_{as}(=CH_3)$
21	3013	ν(=C-H)

ν. stretching; δ. bending; s. symmetric; as. asymmetric

576

577 **Table 2. Fatty acid (FA) composition of the fish meal and fish oil- (FM-FO),**

578 **plant- and commercial-based feeds (% total FA) by FAME-GC analysis.**

	FM-FO feed	Plant-based feed	Commercial feed
12:0	0	0.90	0
14:0	4.96	0.73	1.49
15:0	0.40	0	0.18
16:0	18.22	17.65	9.75
17:0	0.27	0	0.16
18:0	3.30	2.27	1.97
20:0	0.15	0.16	0.29
SFA	27.31	21.71	13.83
16:1	4.18	0.25	1.81
18:1	24.35	39.65	53.02
20:1	1.67	0.36	1.08
22:1	1.10	0	0.22
MUFA	31.46	40.26	56.24
18:2 (LA)	28.57	19.25	19.21
20:4 (ARA)	0.20	0	0.12
PUFA Ω-6	28.77	19.25	19.33
18:3 (ALA)	4.90	18.73	7.41
18:4	1.14	0	0.31
20:5 (EPA)	2.21	0	0.95
22:6 (DHA)	1.99	0	1.15
PUFA Ω-3	10.24	18.73	9.82
PUFA	39.01	37.98	29.15

579

580

581 **Table 3. Fatty acid (FA) composition of the FA from visceral adipose tissues in rainbow**
582 **trout, fed with FM-FO- (N=129), plant- (N=130) or commercial-based (N=9) feeds (%**
583 **total FA) by FAME-GC analysis. The coefficient of variation (CV) was calculated (CV =**
584 **(standard deviation/mean) * 100), and put into brackets.**

	FM-FO feed	Plant-based feed	Commercial feed
12:0	0.06 ± 0.01	0.11 ± 0.02	-
14:0	2.32 ± 0.05	1.67 ± 0.13	3.17 ± 0.33
15:0	0.23 ± 0.01	0.17 ± 0.02	-
16:0	12.60 ± 0.11	12.48 ± 0.48	18.08 ± 1.06
17:0	0.29 ± 0.01	0.23 ± 0.02	-
18:0	3.36 ± 0.01	3.40 ± 0.24	2.32 ± 0.22
20:0	0.23 ± 0.02	0.24 ± 0.02	-
SFA	19.49 ± 0.16 (0.82)	18.71 ± 0.68 (3.63)	24.15 ± 1.33 (5.51)
16:1	3.13 ± 0.13	2.57 ± 0.29	4.27 ± 0.39
18:1	31.66 ± 0.33	36.81 ± 1.04	44.32 ± 1.01
20:1	2.74 ± 0.06	2.08 ± 0.17	1.20 ± 0.31
22:1	2.94 ± 0.06	2.13 ± 0.40	-
MUFA	43.01 ± 0.44 (1.02)	45.72 ± 0.90 (1.97)	49.89 ± 1.05 (2.10)
18:2 (LA)	20.86 ± 0.39 (1.87)	18.90 ± 0.60 (3.17)	15.82 ± 0.66 (4.17)
20:4 (ARA)	0.43 ± 0.07 (16.28)	0.36 ± 0.05 (13.89)	0.17 ± 0.04 (23.53)
PUFA Ω-6	21.76 ± 0.24 (1.10)	19.93 ± 0.62 (3.11)	17.06 ± 0.69 (4.04)
18:3 (ALA)	3.77 ± 0.17 (4.51)	6.29 ± 0.59 (9.38)	4.03 ± 0.18 (4.47)
18:4	0.55 ± 0.08	0.55 ± 0.19	-
20:5 (EPA)	2.29 ± 0.08 (3.49)	1.78 ± 0.19 (10.67)	1.08 ± 0.14 (12.96)
22:6 (DHA)	5.63 ± 0.16 (2.84)	3.94 ± 0.49 (12.43)	1.43 ± 0.56 (39.16)
PUFA Ω-3	13.19 ± 0.13 (0.98)	13.25 ± 0.67 (5.05)	7.54 ± 0.85 (11.27)
PUFA	36.57 ± 0.20 (0.55)	34.58 ± 1.01 (2.92)	24.60 ± 1.28 (5.20)

585

586 **Table 4. Summary statistics of the FA from visceral adipose tissues in rainbow trout**

587 **(N=268), by FAME-GC analysis.**

Fatty acid (FA)	μ^a ($\pm \sigma^b$)	CV[c]	Range (min. - max.)	R^2 [d]	RMSEP[d]
Major FA group					
SFA	19.27 ± 1.22	6.31	16.94 – 26.23	0.42	0.95
MUFA	44.55 ± 1.91	4.29	40.79 – 51.02	0.75	1.04
PUFA	35.23 ± 2.32	6.60	22.82 – 38.98	0.79	1.17
Total Ω-3	13.03 ± 1.19	9.19	6.26 – 15.22	0.66	0.79
Total Ω-6	20.72 ± 1.33	6.42	15.71 – 24.18	0.83	0.56
Individual Ω-9 *FA*					
18:1	37.39 ± 2.82	7.55	32.64 – 45.27	0.85	1.18
20:1	2.50 ± 0.59	23.62	0.00 – 4.21	0.77	0.28
Individual Ω-6 *FA*					
18:2 (LA)	19.74 ± 1.39	7.04	14.73 – 23.26	0.84	0.57
18:3	0.46 ± 0.15	33.35	0.18 – 1.00	0.46	0.11
20:2	0.70 ± 0.41	59.31	0.00 – 1.27	0.04	0.41
20:3	0.47 ± 0.17	35.35	0.00 – 0.84	0.02	0.17
20:4	0.39 ± 0.07	17.69	0.12 – 0.54	0.61	0.05
Individual Ω-3 *FA*					
18:3 (ALA)	5.00 ± 1.32	26.45	3.30 – 7.52	0.82	0.55
18:4	0.52 ± 0.47	90.21	0.00 – 2.30	0,04	0.48
20:5 (EPA)	2.00 ± 0.35	17.60	0.94 – 2.76	0.76	0.18
22:5	0.86 ± 0.14	16.44	0.53 – 1.29	0.44	0.11
22:6 (DHA)	4.66 ± 1.10	23.69	0.80 – 6.45	0.81	0.51
EPA+DHA	6.67 ± 1.43	21.48	1.74 – 8.90	0.82	0.64

[a] μ = mean weight of the % total FA for all samples used within investigation
[b] σ = standard deviation of the % total FA
[c] CV = coefficient of variation (SD /mean*100).
[d] R^2 and RMSECV = statistical values from the ridge regression methods for the calibration

588

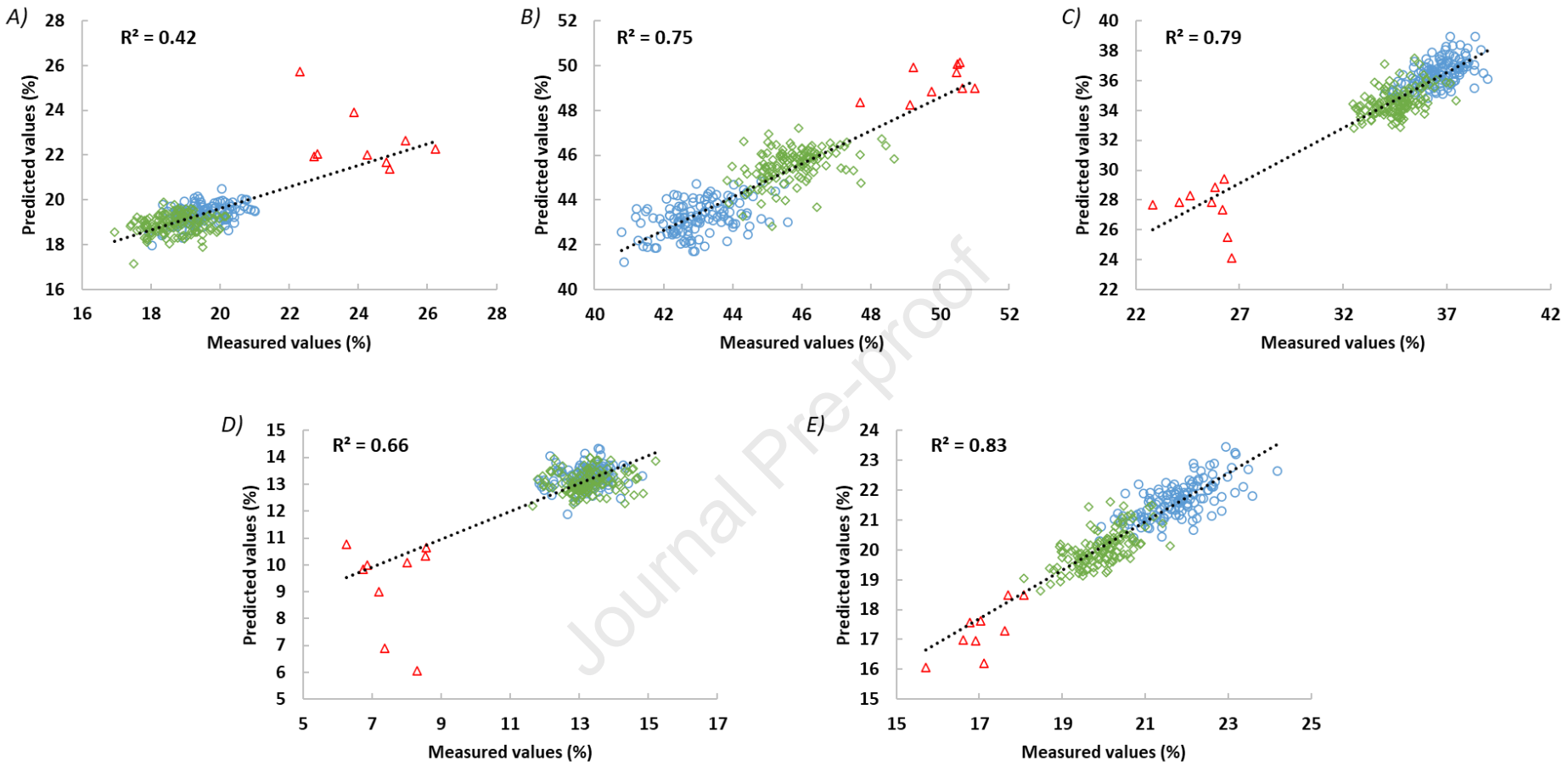

589

590 **Fig. 3. Predicted values using Raman spectra compared to measured values by using ridge regression, for each major FA group. (A)**

591 **SFA; (B) MUFA; (C) PUFA; (D) total omega-3; (E) total omega-6. Rainbow trout individuals were fed with a FM-FO- (*blue circle*),**

592 **plant- (*green diamond*), or commercial-based (*red* triangle) feed.**

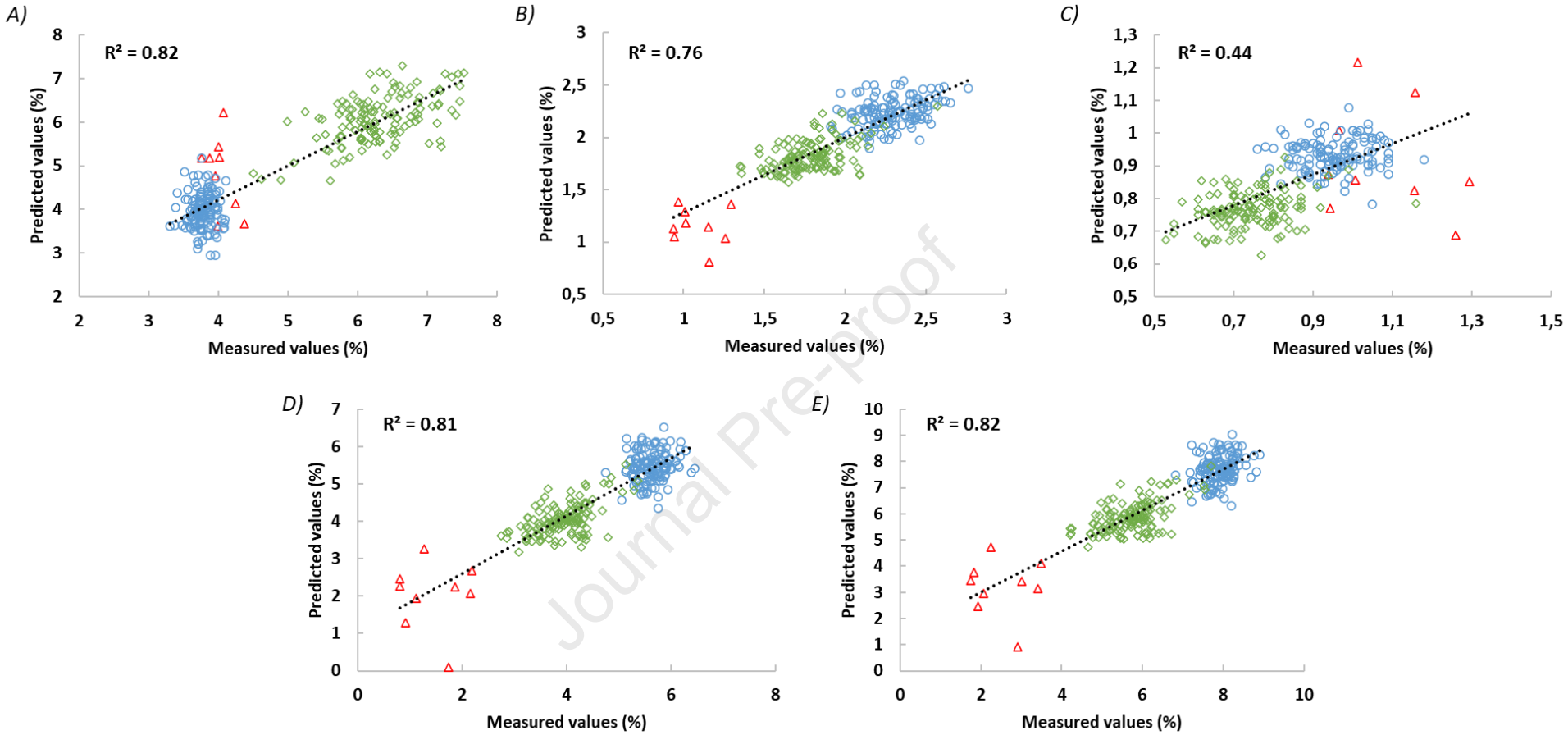

593

594 **Fig. 4. Predicted values using Raman spectra compared to measured values by using ridge regression, for each individual omega-3 FA.**

595 **(A) ALA ; (B) EPA ; (C) 22:5; (D) DHA ; (E) EPA + DHA. Rainbow trout individuals were fed with a FM-FO- (*blue circle*), plant- (*green*

596 ***diamond*), or commercial-based (*red* triangle) feed.**

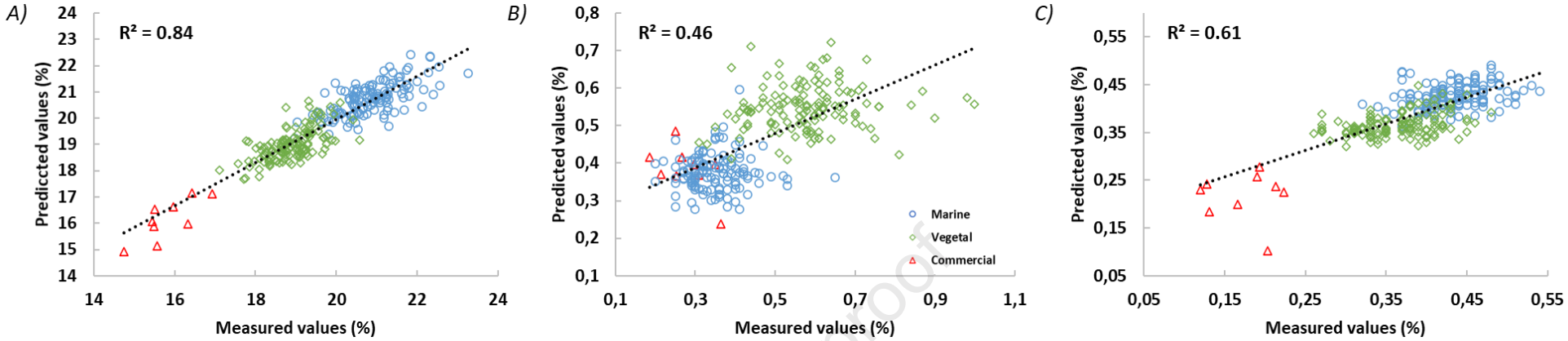

597

598 **Fig. 5. Predicted values using Raman spectra compared to measured values by using ridge regression, for each individual omega-6 FA.**

599 **(A) LA; (B) 18:3; (C) 20:4. Rainbow trout individuals were fed with a FM-FO- (*blue circle*), plant- (*green diamond*), or commercial-based**

600 **(*red* triangle) feed.**

601

Highlights

- Fatty acids composition was predicted in rainbow trout *Onchorhynchus mykiss*.
- Three different feeds allowed to obtain different fatty acids composition.
- Raman spectroscopy was used to analyze adipose tissues from rainbow trout.
- Ω-3 eicosapentaenoic and docosahexenoic fatty acids have great R^2 values.
- Calibration models can be used for large scale and high throughput phenotyping.

Declaration of interests

☒ The authors declare that they have no known competing financial interests or personal relationships that could have appeared to influence the work reported in this paper.

☐The authors declare the following financial interests/personal relationships which may be considered as potential competing interests: